

## Scattering from dielectrically coated bodies of revolution with attached wires<sup>\*</sup>

Akeel S. Tahir<sup>3</sup>, Wa'il A. Godaymi (Ph. D)<sup>1</sup>, and Ahmad H. Abood (Ph. D)<sup>2</sup>

<sup>(1)</sup> Physics Dept., College of Science, Basra University, Basra, Iraq.

<sup>(2)</sup> College of Science, Misan University, Misan, Iraq.

<sup>(3)</sup> Corresponding Author: Akeel S. Tahir, Physics Dept., College of Science, Basra University

**Keyword:-** Dielectrically Coated Body Of Revolution (DBOR) , Attached Wires, Junction

### ABSTRACT

In this work, the electromagnetic (EM) scattering from dielectrically coated bodies of revolution (DCBOR) with attached wires is presented. The equivalent principle is used to generate the surface integral equation (SIE) formulations for the problem, which introduces by the surface electric current density on the conducting surface and both electric and magnetic surface current densities on the dielectric surface. The method of moments (MoM) with Galerkin approach is used to solve the resulting system of integral equations (IEs).

The choice of DCBOR with attached electrical wires as the scatterer, came from the importance of the application used in this research, which representing a proposed model of irregular shape and partially coated ( just in BOR region).

Numerical results for the scattering from this model by using partially coated of the radar absorbing materials (RAM) include complex parameters ,electric permittivity  $\epsilon$  and magnetic permeability  $\mu$ , for electric and magnetic absorbing materials, was a good check for radar cross section reduction (RCSR) in a partial coated for complex proposed model. Where this method has proven its efficiency in reducing and distortion the RCS pattern.

---

(\*) This paper is unsheathed from Ph. D thesis entitled " RADAR CROSS SECTION PREDICTION AND REDUCTION FROM BODIES OF REVOLUTION WITH ATTACHED WIRES" submitted to the Physics Dept., College of Science, Basrah University

(1) Physics Dept., College of Science, Basra University, Basra, Iraq, [wailcomm@yahoo.com](mailto:wailcomm@yahoo.com)

(2) College of Science, Misan University, Missan, Iraq, [prof,dr,ahmad@uomisan.edu.iq](mailto:prof,dr,ahmad@uomisan.edu.iq)

(3) Corresponding Author: Akeel S. Tahir, Physics Dept., College of Science, Basra University, Basra, Iraq, [akeelsami34@yahoo.com](mailto:akeelsami34@yahoo.com)

## الاستطارة الكهرومغناطيسية من الاجسام المتناظرة محوريا المطلية بالعازل والمثبت عليها الاسلاك

### الملحقة

#### الخلاصة

قدم هذا العمل الاستطارة الكهرومغناطيسية من الاجسام الموصلة المتناظرة محوريا والمطلية بالمادة العازلة مع الاسلاك الملحقة. استخدم مبدأ التكافؤ لتوليد صيغ المعادلات التكاملية السطحية للمسألة، والتي عُرفت بواسطة كثافة التيار السطحي الكهربائي على السطح الموصل وكثاقتي التيار الكهربائي والمغناطيسي على السطح العازل. استخدمت طريقة العزوم مع تقريب كالركن لحل النظام الناتج للمعادلات التكاملية. أن اختيار الاجسام الموصلة والمطلية بالمادة العازلة مع الاسلاك الملحقة كمستطير، جاء من اهمية التطبيق المستخدم في هذا البحث، والذي مثله النموذج المقترح غير منتظم الشكل والمطلي جزئيا (الطلاء فقط للجسم المتناظر). أن النتائج العددية للاستطارة من هذا النموذج باستخدام الطلاء الجزئي للمواد الماصة لاشعة الرادار والمحتوية على المركبات العقدية للسماحية الكهربائية  $\epsilon$  والنفاذية المغناطيسية  $\mu$  كانت تأكيد جيد لتقليل مساحة المقطع الراداري بواسطة الطلاء الجزئي للنموذج المعقد المقترح. حيث اثبتت هذه الطريقة كفاءتها في تقليل وتشويه هيكل المقطع الراداري.

## INTRODUCTION

The problem of EM scattering from conducting objects coated by the dielectrics has been studied extensively and many publications are available for this problem. These studies have been motivated not solely by academic interest but by many engineering applications as well.

The coated considerations interest are of practical importance, for example, in radar camouflage, where the coating might be used to minimize or maximize the scattering, and in scattering measurement, where the coating can reduce the influence of the supports on the test object [1]. However, most of earlier techniques have been utilized to solve two and three-dimensional BOR [2][3].

Recently, the study of the EM scattering from conducting objects coated with thin electric or magnetic materials has been the subject of intense investigation. Proper selection of the coating material can be used to reduce significantly radar cross section (RCS) of the coated objects [4]. It is known that the RCS of a conducting body can be reduced if it is coated with absorbing materials especially with anisotropic radar absorbing materials (RAM) [5]. Moreover, coated by thin-layer material has received much attention because these composite dielectric and conductor structures are used in many applications, such as the evaluation of echo from stealth aircraft [6].

Various numerical techniques, such as the method of moment MoM, and formulations of SIEs have been used to treat the problem of conducting objects coated with electric and/or magnetic materials. The general SIE formulations are valid for arbitrary coating thicknesses and these formulations have been used to treat conducting objects with thin or thick coatings. These formulations require careful calculation of the matrix elements when the coating thickness approaches zero [4]. Also the use of these formulations requires a large matrix size. The integral equation used in [7] for the analysis of arbitrarily shaped 3D coated structure is the combination of the electric field integral equation (EFIE) and the PMCHWT (Poggio-Miller-Chang- Harrington-Wu-Tsai) formulation. Kishk and Shafai [2] developed five different formulations, including the combined field integral equation (CFIE) formulation in which the electric and magnetic fields have been used, for multi BORs. In general, imposition of the tangential boundary condition on both the electric and magnetic fields on the coating and on the conducting surface ensures a well-posed formulation. The PMCHWT approach addresses the coating, while the CFIE formulation in [8] is a satisfactory remedy at the conductor.

In this paper the composite dielectric and conductor structures with attached thin electric wires are presented here, where the junction region located between the wires and dielectric bodies of revolution (DBOR) surface as shown in Fig.(1) and (2). By observing the shape regions, we find that the EFIE-PMCHWT formulations are possible to apply between DBOR and wires. correspondingly, the CFIE-PMCHWT formulations are possible to apply between the composite dielectric and conductor structures.

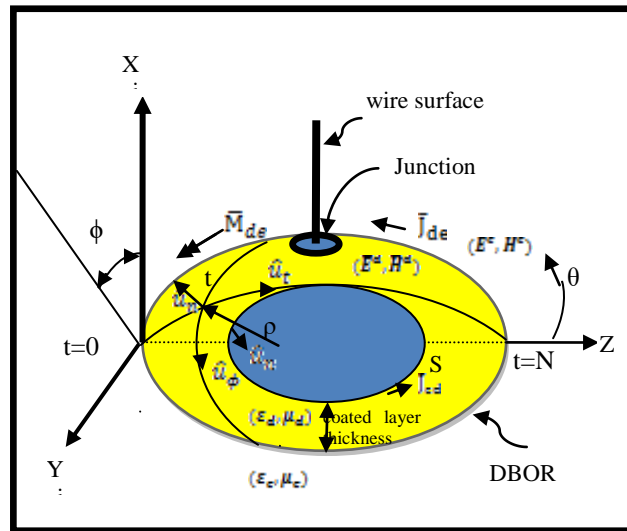


**Fig.(1): The structure under test**

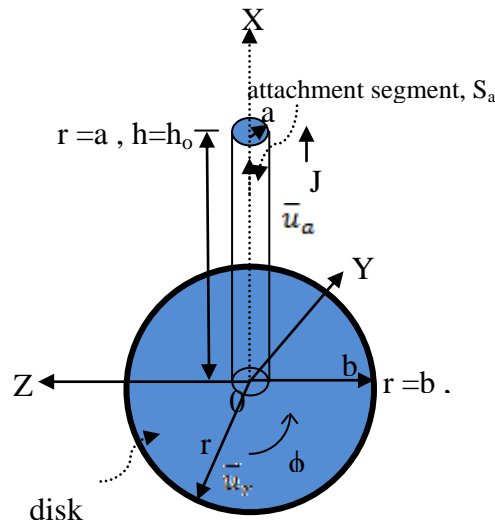


**Fig.(2): Attachment region at the wire/BOR surface.**

### Formulation of the boundary value problem

The formulations are present by using SIEs to analyze the dielectrically coated bodies of revolution (DCBOR) with attached thin electric wire and junction at the wire/DBOR surface. For the purpose of presentation, we assume that the conducting body enclosed by a homogeneous dielectric material. The DCBOR are represented as the cross section of a surface of revolution,  $S_{de}$  and  $S_{cd}$ , respectively. The regions on the exterior and interior of the dielectric body, enclosing a conductor, are characterized by constitutive parameters  $(\epsilon_e, \mu_e)$  and  $(\epsilon_d, \mu_d)$ , respectively. The thin electric wire can be represented by one dimensional structure, on compliance with the well-known thin wire theory [9], and the wire elements are characterized by  $S_{wd}$  and  $S_{we}$  with respect to the interior and exterior to the DBOR. The same concept applies to the junction region, which is represented by  $S_{jd}$  and  $S_{je}$ . The complex structure

(DCBOR-wire-junction) is illuminated by an incident plane wave, of which the electric and magnetic fields are denoted by  $E^i$  and  $H^i$ . The equivalent electric and magnetic surface currents, which arise from application of the field equivalence principle [10] on the exterior and interior region of Fig.(3a), are represented by the symbols  $\bar{J}$  and  $\bar{M}$ , respectively. From this principle two equivalent problems, interior and exterior, are illustrated in Figs.(3b) and (3c), respectively. The field components in each region can therefore be found readily from these equivalent currents, these equivalent currents are still unknown and can be determined by enforcing the boundary conditions for the field vectors in Fig.(3a). The boundary conditions to be satisfied are:-

$$\hat{n} \times \bar{E}^{et} = 0 \quad (1a)$$

$$\hat{n} \times \bar{H}^{et} = 0 \quad (1b)$$

$$\hat{n} \times \bar{E}^{dt} = 0 \quad (1c)$$

$$\hat{n} \times \bar{H}^{dt} = 0 \quad (1d)$$

The electric and magnetic field vectors are represented by the symbols  $\bar{E}$  and  $\bar{H}$  with superscripts "dt" and "et" refer to the total field interior and exterior to the DCBOR, respectively.

The surface equivalent currents are:

$$\bar{J}_{we} = \hat{n} \times \bar{H}^e, \text{ on } S_{we} \quad (2a)$$

$$\bar{J}_{wd} = \hat{n} \times \bar{H}^d, \text{ on } S_{wd} \quad (2b)$$

$$\bar{J}_{je} = \hat{n} \times \bar{H}^e, \text{ on } S_{je} \quad (2c)$$

$$\bar{J}_{jd} = \hat{n} \times \bar{H}^d, \text{ on } S_{jd} \quad (2d)$$

$$\bar{J}_{cd} = \hat{n} \times \bar{H}^d, \text{ on } S_{cd} \quad (2e)$$

$$\bar{J}_{de} = \hat{n} \times \bar{H}^e, \text{ on } S_{de} \quad (2f)$$

$$\bar{M}_{de} = -\hat{n} \times \bar{E}^e, \text{ on } S_{de} \quad (2g)$$

By enforcing the continuity of the tangential components of the total electric and magnetic fields on  $S_{cd}$ ,  $S_{de}$ ,  $S_{we}$ ,  $S_{wd}$ ,  $S_{je}$ , and  $S_{jd}$  regions, from which the unknown  $\bar{J}_{wd}$ ,  $\bar{J}_{we}$ ,  $\bar{J}_{jd}$ ,  $\bar{J}_{je}$ ,  $\bar{J}_{cd}$ ,  $\bar{J}_{de}$  &  $\bar{M}_{de}$  can be determined. A system of integro-differential equations can be obtained and written in operator form as [2][11]:

$$\bar{E}_{\tan}^d (\bar{J}_{de} + \bar{J}_{cd} + \bar{J}_{wd} + \bar{J}_{jd}, \bar{M}_{de}) = \bar{E}_{\tan}^{id}, \text{ on } S_{wd} \text{ and } S_{jd} \quad (3a)$$

$$\bar{E}_{\tan}^e (\bar{J}_{de} + \bar{J}_{we} + \bar{J}_{je}, \bar{M}_{de}) = -\bar{E}_{\tan}^{ie}, \text{ on } S_{we} \text{ and } S_{je} \quad (3b)$$

$$\bar{E}_{\tan}^d(\bar{J}_{de} + \bar{J}_{cd}, \bar{M}_{de}) = \bar{E}_{\tan}^{id} \quad , \text{ on } S_{cd}$$

(3c)

$$\bar{E}_{\tan}^e(\bar{J}_{de} + \bar{J}_{we} + \bar{J}_{je}, \bar{M}_{de}) + \bar{E}_{\tan}^d(\bar{J}_{de} + \bar{J}_{cd} + \bar{J}_{wd} + \bar{J}_{jd}, \bar{M}_{de}) = \bar{E}_{\tan}^{id} - \bar{E}_{\tan}^{ie} \quad , \text{ on } S_{de}$$

(3d)

$$\bar{H}_{\tan}^e(\bar{J}_{de} + \bar{J}_{we} + \bar{J}_{je}, \bar{M}_{de}) + \bar{H}_{\tan}^d(\bar{J}_{de} + \bar{J}_{cd} + \bar{J}_{wd} + \bar{J}_{jd}, \bar{M}_{de}) = \bar{H}_{\tan}^{id} - \bar{H}_{\tan}^{ie} \quad , \text{ on } S_{de}$$

(3e)

The subscript (tan) denotes the tangential components of the fields on the surface in equation.  $\bar{E}^a(\bar{J}, \bar{M})$  and  $\bar{H}^a(\bar{J}, \bar{M})$  are the electric and magnetic fields due to the equivalent electric and magnetic currents  $\bar{J}$  and  $\bar{M}$  radiating in the homogeneous medium characterized by  $\mu_a$  and  $\epsilon_a$  everywhere. The superscripts (a) represents (e) or (d).

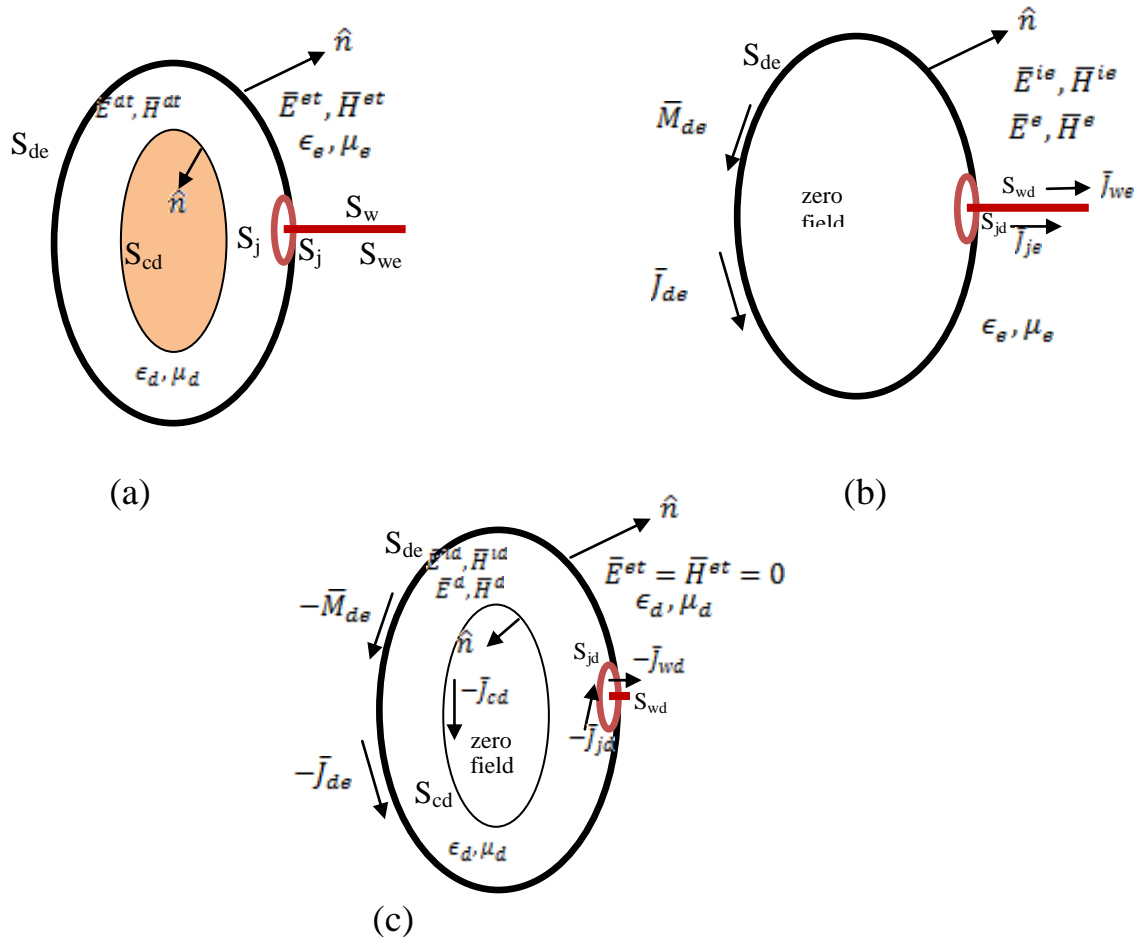


**Fig.(3): (a) The original problem, (b) The interior problem and (c) The exterior problem.**

As mentioned the CFIE-PMCHWT formulations can be applied between the composite dielectric and conductor structures, and EFIE-PMCHWT formulations can be applied between DBOR and wires. These formulas are possible to explain briefly

by place of application. The combined of E- and H-field formulations suffer from the resonance problem, similar to the formulations for the conducting bodies [8]. To overcome the problem in the composite dielectric and conductor structures, a linear combination of the E- and H-field formulations may be obtained to give [2]:

$$\hat{n} \times \bar{H}^d(\bar{J}_{cd} + \bar{J}_{ds}, \bar{M}_{ds}) - \frac{\alpha^d}{\eta_d} \bar{E}_{tan}^d \times (\bar{J}_{cd} + \bar{J}_{ds}, \bar{M}_{ds}) = 0 \quad \text{just outside } S_{cd} \quad (4)$$

$$\hat{n} \times \bar{H}^d(\bar{J}_{cd} + \bar{J}_{ds}, \bar{M}_{ds}) - \frac{\alpha^d}{\eta_d} \bar{E}_{tan}^d \times (\bar{J}_{cd} + \bar{J}_{ds}, \bar{M}_{ds}) = 0 \quad \text{just outside } S_d \quad (5)$$

$$\hat{n} \times \bar{H}^e(\bar{J}_{ds}, \bar{M}_{ds}) - \frac{\alpha^e}{\eta_e} \bar{E}_{tan}^e \times (\bar{J}_{ds}, \bar{M}_{ds}) = \hat{n} \times \bar{H}^e(\bar{J}^{ie}, \bar{M}^{ie}) - \frac{\alpha^e}{\eta_e} \bar{E}_{tan}^e \times (\bar{J}^{ie}, \bar{M}^{ie})$$

just inside  $S_{de}$  (6)

Kishk and Shafai [2] proved that the results, EFIE-PMCHWT and combined field formulations for coated conductors, are very closed in comparison with exact analytical solutions (Mie series). So, in this paper, for coated conductors, we define "EFIE-PMCHWT" the formulation that utilizes an E-field on the conductor and a PMCHWT on the dielectric consistent with DBOR-wires.

The scattering of EM waves from coated conductors object having permeability  $\epsilon_d$  and permeability  $\mu_d$  with a homogeneous background medium ( $\epsilon_e, \mu_e$ ) as shown in Fig.(1), can be expressed in terms of integro-differential operator according to PMCHWT formulation [12], the boundary condition on  $S_{de}$  imply:

$$\bar{E}_{tan}^{inc} = [L_1 \bar{J}_1 - K_1 \bar{M}_1 - L_2 \bar{J}_2 + K_2 \bar{M}_2]_{tan} \quad (7)$$

$$\bar{H}_{tan}^{inc} = \left[ K_1 \bar{J}_1 + \frac{1}{\eta_1^2} L_1 \bar{M}_1 - K_2 \bar{J}_2 - \frac{1}{\eta_2^2} L_2 \bar{M}_2 \right]_{tan} \quad (8)$$

Where  $\bar{J}_i$  and  $\bar{M}_i$  are the incident electric and magnetic current densities for region i (i=1,2), also the wave impedance  $\eta_i = \sqrt{\mu_i/\epsilon_i}$ ,  $\bar{E}^{inc}$  and  $\bar{H}^{inc}$  are the incident electric and magnetic field, respectively.

The integro-differential operators  $L_i$  and  $K_i$  are defined as [13]:

$$L_i \bar{X}(\bar{r}) = j\omega\mu_i \int_s \left[ \bar{X}(\bar{r}') + \frac{1}{\omega^2 \mu_i \epsilon_i} \nabla \nabla \cdot \bar{X}(\bar{r}') \right] G_i(|\bar{r} - \bar{r}'|) d\bar{s} \quad (9)$$

$$K_i \bar{X}(\bar{r}) = \int_s \bar{X}(\bar{r}') \times \nabla G_i(|\bar{r} - \bar{r}'|) d\bar{s} \quad (10)$$

where  $\epsilon_i = \epsilon_0 \epsilon_{ir}$ ,  $\mu_i = \mu_0 \mu_{ir}$ , and  $\eta_i = \eta_0 \left( \frac{\mu_{ir}}{\epsilon_{ir}} \right)^{1/2}$ ;  $\epsilon_0$  and  $\mu_0$  are the permittivity and permeability of free space, respectively; and the subscript r denotes the relative constitutive quantity. The Green's function for an unbounded medium is denoted by  $G_i$ , with the constitutive parameters  $\epsilon_i$  and  $\mu_i$ .

## Moment Method Solution

Consider the general geometry of a scatterer made of coated conductors with attached wire as illustrated in Fig.( 1). In the numerical approach of the scattering problem is formulated in terms of the equivalent currents on the surface of the scatterer, leading to a set of integral equations which are solved using the MoM. The

Galerkin procedure is carried out to test boundary integral equations and reduce the functional form of the equations to a partitioned matrix equation.

The DCBOR with attached wires have a system of unknown currents. Due to the axial symmetry of DCBOR, two components of electric and magnetic current can be identified: one directed along the generating arc ( $\hat{u}_t$ ), and the other in the circumferential direction ( $\hat{u}_\phi$ ). The unknown surface current densities are first expanded in terms of Fourier modes [14]

$$\begin{aligned}\bar{J}_s(t, \phi) &= \bar{J}^t(t, \phi) + \bar{J}^\phi(t, \phi) \\ &= \sum_{n=-\infty}^{\infty} [\bar{J}_n^t(t) + \bar{J}_n^\phi(t)] e^{jn\phi} \quad (11a)\end{aligned}$$

$$\begin{aligned}\bar{M}_s(t, \phi) &= \eta_a (\bar{M}^t(t, \phi) + \bar{M}^\phi(t, \phi)) \\ &= \eta_a \sum_{n=-\infty}^{\infty} [\bar{M}_n^t(t) + \bar{M}_n^\phi(t)] e^{jn\phi} \quad (11b)\end{aligned}$$

Where  $\eta_a$  is the wave impedance for interior or exterior regions.

These components can be further expanded on the generating arc in terms of sub-domain basis functions  $f_i$  as:

$$\left. \begin{aligned}\bar{J}_n^t(t) &= \hat{u}_t \sum_{i=1}^{N_s-1} I_{ni}^t f_i(t) \\ \bar{J}_n^\phi(t) &= \hat{u}_\phi \sum_{i=1}^{N_s-1} I_{ni}^\phi f_i(t)\end{aligned} \right\} \quad (12a)$$

$$\left. \begin{aligned}\bar{M}_n^t(t) &= \hat{u}_t \sum_{i=1}^{N_s-1} k_{ni}^t f_i(t) \\ \bar{M}_n^\phi(t) &= \hat{u}_\phi \sum_{i=1}^{N_s-1} k_{ni}^\phi f_i(t)\end{aligned} \right\} \quad (12b)$$

Where  $N_s$  represent  $N_c$  or  $N_d$ , the  $f_i(t) = \frac{1}{\rho} T_i(t)$  and  $T_i$  is the triangular function as shown in Fig.(4a). The testing function is

$$\bar{W}_{mi}^\alpha = \hat{u}_\alpha f_i(t) e^{-jm\phi}, \quad \alpha=t \text{ or } \phi \quad (13)$$

For wire, the basis  $\bar{J}^w$  and testing functions  $\bar{W}^w$  are introduced by [15]

$$\bar{J}^w = \hat{u}_\ell^w I_\ell^w T_\ell(h) = \sum_{\ell=1}^{N_w-1} \hat{u}_\ell^w I_\ell^w T_\ell(h) \quad (14)$$

$$\bar{J}^w = \bar{W}^w \quad (15)$$

Where  $\hat{u}_\ell^w$  is the unit vector along wire segment, and  $T_\ell(h)$  is the triangular function as shown in Fig.(4b).

The junction basis  $\bar{J}^j$  and testing functions  $\bar{W}^j$  have the form

$$\bar{J}^j(p) = I^j \begin{cases} J_a^j, & p \in S_a \\ J_d^j, & p \in S_d \end{cases} \quad (16a)$$

Where

$$\bar{J}_a^j = \hat{u}_a \frac{T_a(h)}{2\pi a} \quad (16b)$$

$$\bar{J}_d^j = -\hat{u}_r \frac{1}{2\pi r} \left( \frac{b-r}{b-a} \right) \quad (16c)$$

$$\bar{J}^j = \bar{W}^j \quad (17)$$

Where  $\bar{J}_a^j$  is the current density on the wire segment nearest the junction region, i.e., wire attachment segment  $S_a$ ,  $\bar{J}_d^j$  is the current density over the BOR surface near the junction regions (disk region)  $S_d$ ,  $\hat{u}_a$  and  $T_a(h)$  are an outward-directed unit vector and half-triangle function as shown in Fig.(4c) on the attachment segment, respectively;  $\hat{u}_r$  is a unit vector on the (annular) disk surface away from the wire,  $r$  is the radial distance on the disk,  $b$  is the outer disk radius,  $a$  is the wire radius as shown in Fig.(2). A similar formulation for the junction currents is given in [15] and [16].

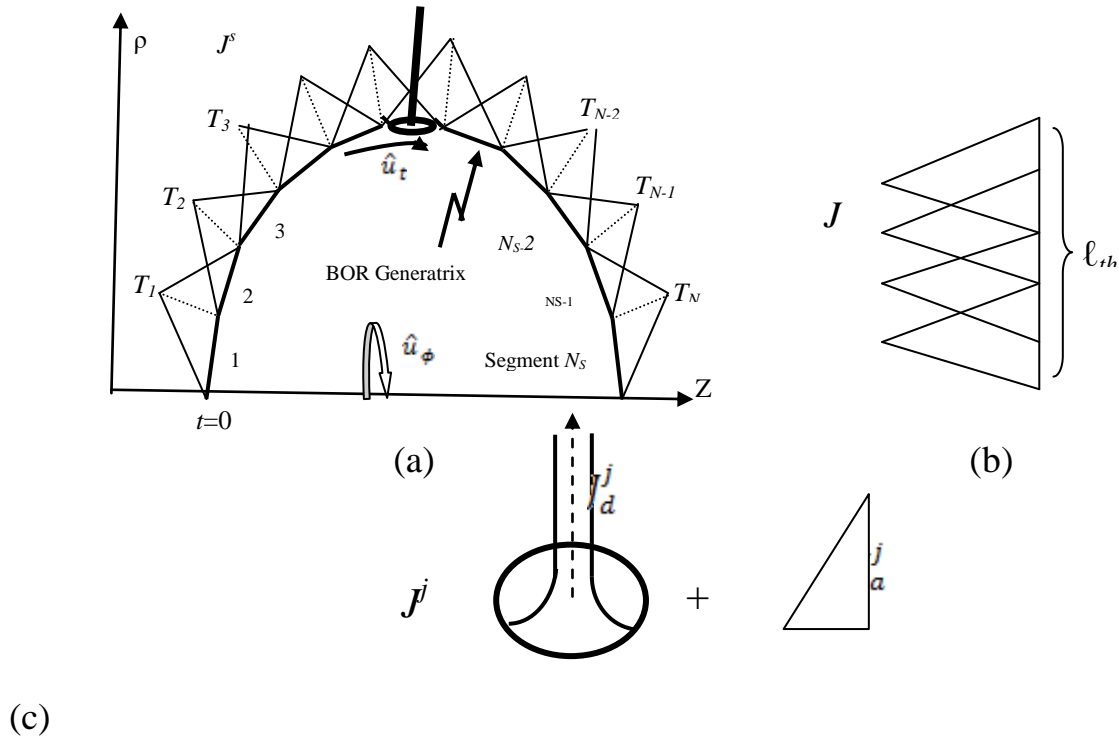


Fig.(4): Triangular basis functions (a) over the BOR generatrix.(b) on  $l_{th}$  segment of attachment wire. (c) junction region representation.

The number of data points on the CBOR, DBOR wire and junction region are  $N_c$ ,  $N_d$ ,  $N_w$  and  $N_a$ , respectively. The scattered is thus modeled by adding the four region data points [17]. Then, The total number of data points are  $N = N_c + N_d + N_w + N_a$ .

All the unknowns ( $I_{ni}^t, I_{ni}^\phi, k_{ni}^t, k_{ni}^\phi, I^w$ , and  $\bar{J}$ ), which defined with basis function in Eqs.( 12), (14), and (16), are Possible to give Eq.(3) the following forms:

$$\left. \begin{aligned}
 & \sum_{n=-\infty}^{\infty} \left[ \sum_{j=1}^{N_d-1} I_{nj} \bar{E}_{\tan}^d(\bar{J}_j^d, 0) + \sum_{j=1}^{N_c-1} I_{nj}^c \bar{E}_{\tan}^d(\bar{J}_j^c, 0) + \sum_{l=1}^{N_w-1} I_{lj}^w \bar{E}_{\tan}^d(\bar{J}_l^w, 0) + \right. \\
 & \left. \sum_{j=1}^{N_a-1} I_j^{jd} \bar{E}_{\tan}^d(\bar{J}_j^d, 0) + \eta_d \sum_{j=1}^{N_d-1} K_{nj} \bar{E}_{\tan}^d(0, \bar{M}_{nj}) \right] = \bar{E}_{\tan}^{id}(\bar{J}^d)
 \end{aligned} \right\} \text{on } S_{wd} \text{ and } S_{jd}$$

(18a)

$$\left. \begin{aligned} & \sum_{n=-\infty}^{\infty} \left[ \sum_{j=1}^{N_d-1} I_{nj} \bar{E}_{\tan}^e(\bar{J}_{nj}^e, 0) + \sum_{l=1}^{N_w-1} I_l^{we} \bar{E}_{\tan}^e(\bar{J}_w^e, 0) \right. \\ & \left. + \sum_{j=1}^{N_a-1} I_j^{je} \bar{E}_{\tan}^e(\bar{J}_j^e, 0) + \eta_e \sum_{j=1}^{N_d-1} K_{nj} \bar{E}_{\tan}^e(0, \bar{M}_{nj}) \right] = \bar{E}_{\tan}^{ie}(\bar{J}^e) \end{aligned} \right\} \text{ on } S_{we} \text{ and } S_{je}$$

(18b)

$$\sum_{n=-\infty}^{\infty} \left[ \sum_{j=1}^{N_d-1} I_{nj} \bar{E}_{\tan}^d(\bar{J}_{nj}^d, 0) + \sum_{j=1}^{N_c-1} I_{nj}^c \bar{E}_{\tan}^d(\bar{J}_{nj}^c, 0) + \eta_d \sum_{j=1}^{N_d-1} K_{nj} \bar{E}_{\tan}^d(0, \bar{M}_{nj}) \right] = \bar{E}_{\tan}^{id}(\bar{J}^d) \text{ on } S_{cd}$$

(18c)

$$\left. \begin{aligned} & \sum_{n=-\infty}^{\infty} \left[ \sum_{j=1}^{N_d-1} I_{nj} \{ \bar{E}_{\tan}^d(\bar{J}_{nj}^d, 0) + \bar{E}_{\tan}^e(\bar{J}_{nj}^e, 0) \} + \sum_{j=1}^{N_c-1} I_{nj} \bar{E}_{\tan}^d(\bar{J}_{nj}^c, 0) + \right. \\ & \left. \sum_{l=1}^{N_w-1} \{ I_l^{wd} \bar{E}_{\tan}^d(\bar{J}_w^d, 0) + I_l^{we} \bar{E}_{\tan}^e(\bar{J}_w^e, 0) \} + \sum_{j=1}^{N_a-1} \{ I_j^{jd} \bar{E}_{\tan}^d(\bar{J}_j^d, 0) + I_j^{je} \bar{E}_{\tan}^e(\bar{J}_j^e, 0) \} \right\} \text{ on } S_{de} \\ & + \sum_{j=1}^{N_d-1} K_{nj} \{ \eta_d \bar{E}_{\tan}^d(0, \bar{M}_{nj}) + \eta_e \bar{E}_{\tan}^e(0, \bar{M}_{nj}) \} = \bar{E}_{\tan}^{id}(\bar{J}^d) - \bar{E}_{\tan}^{ie}(\bar{J}^e) \end{aligned} \right\}$$

(18d)

$$\left. \begin{aligned} & \sum_{n=-\infty}^{\infty} \left[ \sum_{j=1}^{N_d-1} I_{nj} \{ \bar{H}_{\tan}^d(\bar{J}_{nj}^d, 0) + \bar{H}_{\tan}^e(\bar{J}_{nj}^e, 0) \} + \sum_{j=1}^{N_c-1} I_{nj} \bar{H}_{\tan}^d(\bar{J}_{nj}^c, 0) \right. \\ & \left. + \sum_{l=1}^{N_w-1} \{ I_l^{wd} \bar{H}_{\tan}^d(\bar{J}_w^d, 0) + I_l^{we} \bar{H}_{\tan}^e(\bar{J}_w^e, 0) \} + \sum_{j=1}^{N_a-1} \{ I_j^{jd} \bar{H}_{\tan}^d(\bar{J}_j^d, 0) + I_j^{je} \bar{H}_{\tan}^e(\bar{J}_j^e, 0) \} \right\} \text{ on } S_{de} \\ & + \sum_{j=1}^{N_d-1} K_{nj} \{ \eta_d \bar{H}_{\tan}^d(0, \bar{M}_{nj}) + \eta_e \bar{H}_{\tan}^e(0, \bar{M}_{nj}) \} = \bar{H}_{\tan}^{id}(\bar{J}^d) - \bar{H}_{\tan}^{ie}(\bar{J}^e) \end{aligned} \right\}$$

(18e)

The dot product between Eq.(4-11) and the weighting functions, Galerkin approach, in Eqs.(13), (15), and (17), and this gives a system of linear equation has the form:

$$[ I ] [ Z ] = [ V ] \quad (19)$$

and in more details it can be written in matrix form as follow:

$$\begin{bmatrix} [Z_{cd,cd}]_n & [Z_{cd,d\epsilon}]_n & \eta_r [V_{cd,d\epsilon}]_n & [0] & [0] & [0] & [0] \\ [Z_{de,cd}]_n & ([Z_{de,d\epsilon}]_n + \eta_r [Z_{de,d\epsilon}^d]_n) & ([V_{de,d\epsilon}^e]_n + [V_{de,d\epsilon}^d]_n) & \eta_r [Z_{de,wd}]_n & [Z_{de,we}^e]_n & \eta_r [Z_{de,jd}]_n & [Z_{de,je}^e]_n \\ \eta_r [V_{de,cd}]_n & ([V_{de,d\epsilon}^e]_n + [V_{de,d\epsilon}^d]_n) & (-[Z_{de,d\epsilon}^e]_n + \frac{1}{\eta_r} [Z_{de,d\epsilon}^d]_n) & [V_{de,wd}^d]_n & [V_{de,we}^e]_n & [V_{de,jd}^d]_n & [V_{de,je}^e]_n \\ [0] & \eta_r [Z_{wd,d\epsilon}^d]_n & [V_{wd,d\epsilon}^d]_n & [Z_{wd,wd}^d] & [0] & [Z_{wd,jd}^d] & [0] \\ [0] & [Z_{we,d\epsilon}^e]_n & [V_{we,d\epsilon}^e]_n & [0] & [Z_{we,we}^e] & [0] & [Z_{we,je}^e] \\ [0] & \eta_r [Z_{jd,d\epsilon}^d]_n & [V_{jd,d\epsilon}^d]_n & [Z_{jd,wd}^d] & [0] & [Z_{jd,jd}^d] & [0] \\ [0] & [Z_{je,d\epsilon}^e]_n & [V_{je,d\epsilon}^e]_n & [0] & [Z_{je,we}^e] & [0] & [Z_{je,je}^e] \end{bmatrix} \begin{bmatrix} [I^\alpha]_n \\ [I^\alpha]_n \\ [k^\alpha]_n \\ [I^{wd}] \\ [I^{we}] \\ [I^{jd}] \\ [I^{je}] \end{bmatrix} = \begin{bmatrix} [V_{cd}^\alpha]_n^E \\ [V_{de}^\alpha]_n^E \\ [V_{de}^\alpha]_n^H \\ [V^{wd}] \\ [V^{we}] \\ [V^{jd}] \\ [V^{je}] \end{bmatrix}$$

(20)

Where  $\eta_r = \sqrt{\mu_a/\epsilon_a}$  , and  $\alpha = t$  or  $\phi$ . The full representation of the sub matrices of the impedance and admittance and excitation are presented in details in the thesis chapters and appendices.

### The radar cross section evaluation

The far field is the far field scattered by structure of DBOR-wire-junction. For plane wave excitation, and through the reciprocity theorem [14] one may find the radiation field  $\bar{E}^s$  at a distance  $r$  from the origin due to the surface currents  $J$  and  $M$  on  $S$  as,

$$\bar{E}^s \cdot \hat{u}^r = \iint_s (\bar{J}(\bar{r}) \cdot \bar{E}^r - \bar{M}(\bar{r}) \cdot \bar{H}^r) ds \quad (21)$$

Where  $\hat{u}^r$  is a unit vector specifying the polarization,  $\bar{E}^r$  and  $\bar{H}^r$  is the electric and magnetic field is due to  $\hat{u}^r$ , respectively, and given by:

$$\bar{E}^r = -\frac{jk\eta}{4\pi r} e^{-jk r_r} \hat{u}^r e^{-j\bar{k}_r \cdot \bar{r}} \quad (22a)$$

$$\bar{H}^r = -\frac{j}{4\pi r} e^{-jk r_r} (\bar{k}_r \times \hat{u}^r) e^{-j\bar{k}_r \cdot \bar{r}} \quad (22b)$$

Where  $k_r$  is the propagation vector of the plane wave,  $k$  is the propagation constant and  $\eta$  is the intrinsic impedance of the medium outside  $S$ .

In the case of BOR, and for  $\theta$ -polarized plane wave the contribution of measurement matrix  $[R]$  is written by [18]

$$\begin{aligned} (R_n^{t\theta})_i &= \langle \bar{E}_\theta^r, \bar{J}_{ni}^t \rangle \\ (R_n^{\phi\theta})_i &= \langle \bar{E}_\theta^r, \bar{J}_{ni}^\phi \rangle \\ (\mathcal{R}_n^{t\phi})_i &= \langle \bar{H}_\phi^r, \bar{M}_{ni}^t \rangle \\ (\mathcal{R}_n^{\phi\phi})_i &= \langle \bar{H}_\phi^r, \bar{M}_{ni}^\phi \rangle \end{aligned} \quad (23)$$

And for the  $\phi$ -polarized plan wave

$$\begin{aligned} (R_n^{t\phi})_i &= \langle \bar{E}_\phi^r, \bar{J}_{ni}^t \rangle \\ (R_n^{\phi\phi})_i &= \langle \bar{E}_\phi^r, \bar{J}_{ni}^\phi \rangle \\ (\mathcal{R}_n^{t\theta})_i &= -\langle \bar{H}_\theta^r, \bar{M}_{ni}^t \rangle \\ (\mathcal{R}_n^{\phi\theta})_i &= -\langle \bar{H}_\theta^r, \bar{M}_{ni}^\phi \rangle \end{aligned} \quad (24)$$

In other hand side, the contribution to  $R^w$  from the wire in both  $\theta$ -and  $\phi$ -polarized can be written in the form:

$$\begin{aligned} R^{w,\theta} &= \langle \bar{E}_\theta^r, \bar{J}_i^w \rangle \\ R^{w,\phi} &= \langle \bar{E}_\phi^r, \bar{J}_i^w \rangle \end{aligned} \quad (25)$$

Similarly, the contribution to  $R^j$  from the junction are

$$\begin{aligned} R^{j,\theta} &= \langle \bar{E}_\theta^r, \bar{J}_a^j \rangle + \langle \bar{E}_\theta^r, \bar{J}_d^j \rangle \\ R^{j,\phi} &= \langle \bar{E}_\phi^r, \bar{J}_a^j \rangle + \langle \bar{E}_\phi^r, \bar{J}_d^j \rangle \end{aligned} \quad (26)$$

The scattering cross section  $\sigma^{pq}$  is defined by

$$\sigma^{pq} = 4\pi r^2 \frac{|\mathbf{E}_{pq}^s|^2}{|\mathbf{E}^i|^2} \quad (27)$$

Where p is either  $\theta$  or  $\phi$  and q is either  $\theta$  or  $\phi$ ,  $E^i$  and  $E^s$  is the incident and scattered field. For large r the relation between scattering matrix and Eq.(27) can be written as:

$$\sigma^{pq} = 4\pi |S^{pq}|^2 \quad (28)$$

Where

$$S^{pq} = \frac{-j\omega\mu}{4\pi} \left\{ \left[ [R_n^{tp}] [R_n^{\phi p}] [\mathcal{R}_n^{tq}] [\mathcal{R}_n^{\phi q}] \right] \cdot [I_n]^T + \left[ [R^{wp}] [I^{wq}] \right] + \left[ [R^{jp}] [I^{jq}] \right] \right\} \quad (29)$$

So, the RCS in both  $\theta$ - and  $\phi$ -polarized scattered fields can be computed according to [12][15] by:

$$\sigma^{\theta\beta} = \frac{\eta^2 k^4}{16\pi^3} \left\{ \sum_{-\infty}^{\infty} e^{-jn\phi_s} \sum_{i=1}^{N_s-1} \begin{bmatrix} [R_{ni}^{t\theta}] & [-R_{ni}^{\phi\theta}] & [R_{ni}^{t\phi}] & [-R_{ni}^{\phi\phi}] \end{bmatrix} \begin{bmatrix} [I_i^{t\beta}] \\ [I_i^{\phi\beta}] \\ [K_i^{t\beta}] \\ [K_i^{\phi\beta}] \end{bmatrix} \right\}^2 + \sum_{i=1}^{N_w-1} [R_i^{w\theta}] [I_i^{w\beta}] + \sum_{i=1}^{N_a-1} [R_i^{j\theta}] [I_i^{j\beta}] \quad (30)$$

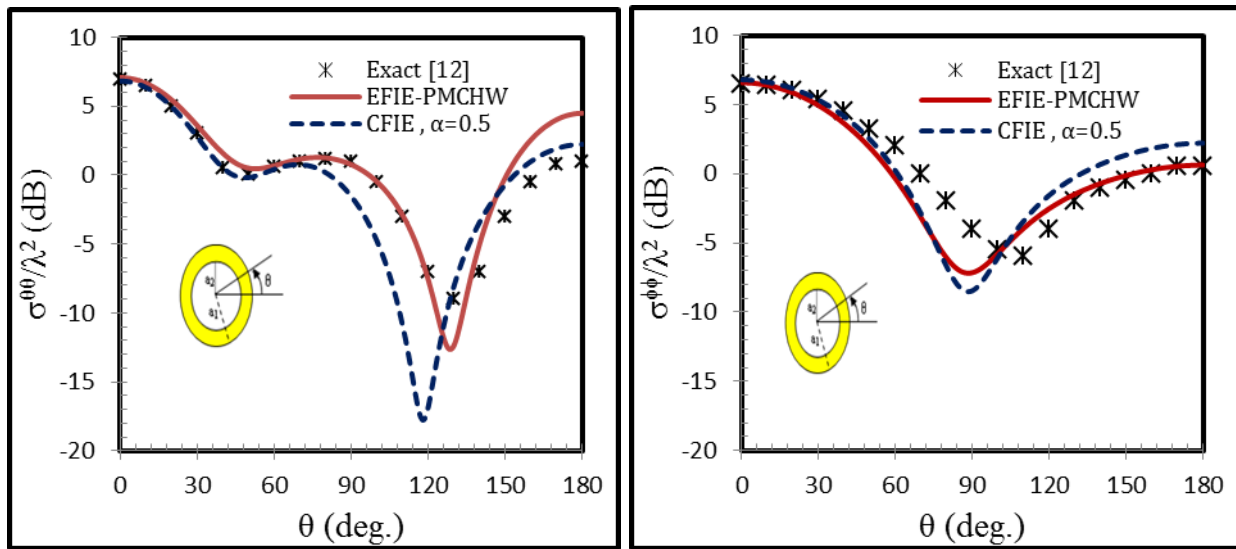
$$\sigma^{\phi\beta} = \frac{\eta^2 k^4}{16\pi^3} \left\{ \sum_{-\infty}^{\infty} e^{-jn\phi_s} \sum_{i=1}^{N_s-1} \begin{bmatrix} [R_{ni}^{t\phi}] & [-R_{ni}^{\phi\phi}] & [-R_{ni}^{t\theta}] & [R_{ni}^{\phi\theta}] \end{bmatrix} \begin{bmatrix} [I_i^{t\beta}] \\ [I_i^{\phi\beta}] \\ [K_i^{t\beta}] \\ [K_i^{\phi\beta}] \end{bmatrix} \right\}^2 + \sum_{i=1}^{N_w-1} [R_i^{w\phi}] [I_i^{w\beta}] + \sum_{i=1}^{N_a-1} [R_i^{j\phi}] [I_i^{j\beta}] \quad (31)$$

Where  $\beta = \theta$  or  $\phi$

## Results

The validity of the computational procedure was first verified. The numerical solution using the present method is compared with the exact solution for the coated sphere, using Mei series [12]. Figure (5) shows the bistatic radar cross section (RCS) in  $\theta\theta$ - and  $\phi\phi$ -polarized of coated conducting sphere for radius  $a_1 = 0.394 \lambda$ ,  $a_2 = 0.311\lambda$ , where the excitation is due to a plane wave incident from the direction of  $\theta = 180^\circ$ . It was shown from this figure that the agreement between both solutions, CFIE

and EFIE-PMCHW, is very good with exact solution [12] for a coating thickness equal to  $0.083\lambda$  and  $\epsilon_r = 2$ .



(a)  $\theta\theta$ - polarized

(b)  $\phi\phi$ -polarized

**Fig.(5): computed bistatic cross section for conducting sphere ( $a_2=0.311\lambda$ ) coated with homogeneous dielectric ( $a_1 = 0.394 \lambda$ , and  $\epsilon_r =2$ ): comparison of the generalized CFIE, EFIC-PMCHWT, and Mie solutions.**

To illustrate the properties and behavior of the present generalized EFIE-PMCHWT formulations, which solve by MoM, next some results for perfectly conducting scatterers coated with a single homogeneous layer of dielectric material with attached wires are presented. Three applications are considered: (a) coated sphere with one attached wire, (b) coated flat-faced cylinder with two attached wires, and (c) coated rocket with four electric wings (partially coated for irregular object), the coated just for BOR. Because of the results has no previously been described, all applications depend on the comparisons of the results of conductor BOR with attached wires (which compared with measurement data of [19]) to demonstrate the effected of coated technique on the total RCS pattern. Note, the junction dimensions for all applications are  $a=0.005\lambda$  and  $b=0.107\lambda$ .

The first application, conducting sphere of radius  $a=0.444\lambda$ , enclosed by a single layer of dielectric material with thickness  $t=0.083\lambda$  and  $\epsilon_r=4$ . coated sphere attached with electric wire of length  $l_w=0.444\lambda$ . The horizontal polarization (HP) backscattered cross sections for complex structures ,conductor body with attached wires and coated body with attached wires, are shown in Figures.(6) and (7). The results proved that the decline in RCS can be very clear in comparison with the case of the conductor body. Furthermore, the effect of wire stays at angles  $\theta > 90^\circ$  and the number of folds are in decreased.

To identify the second application, Figures.(8) and (9) shows the HP monostatic RCS of a conducting and coated flat-faced cylinder, respectively. The dielectric material of thickness  $t=0.083\lambda$  and  $\epsilon_r=4$ , where the cylinder radius  $a=0.344\lambda$  and length  $l_c=1.98\lambda$ . coated cylinder attached with two electric wires located at the center of cylinder and have equal length  $l_{w1}=l_{w2}=0.880\lambda$ . It is clear in Figures that the decline in RCS will be at the ends of the pattern, and in main lobe, and equal effect for both wires at the pattern sides of total RCS .

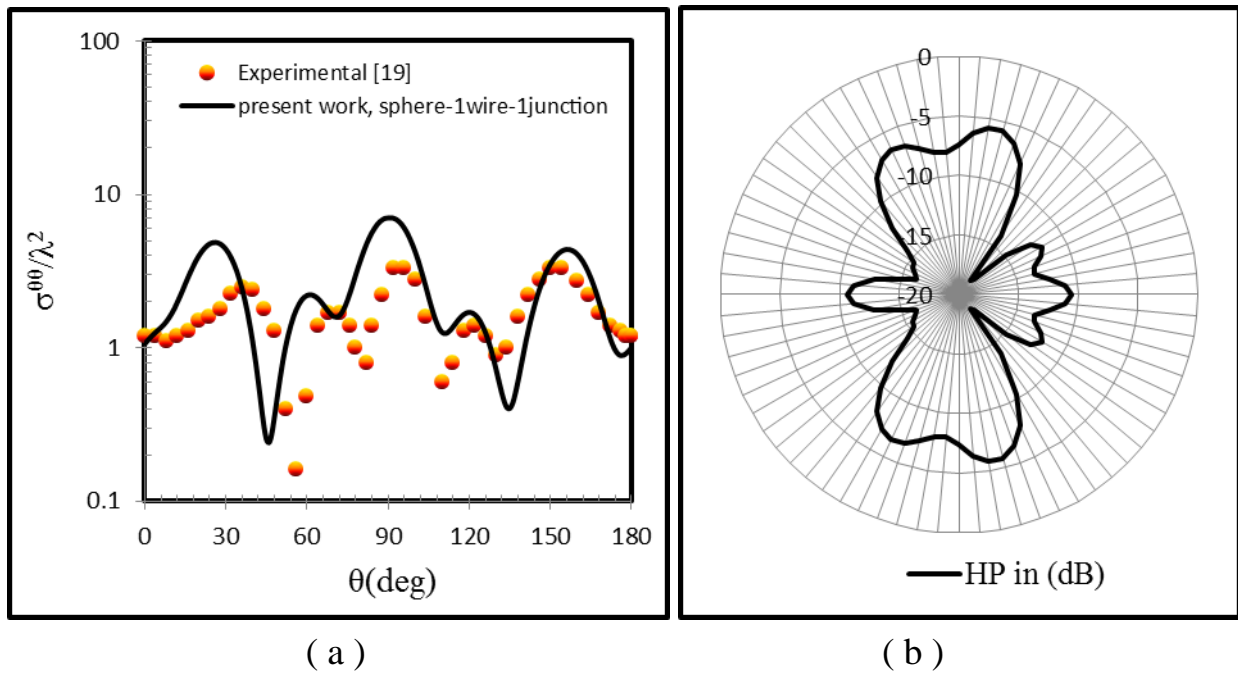
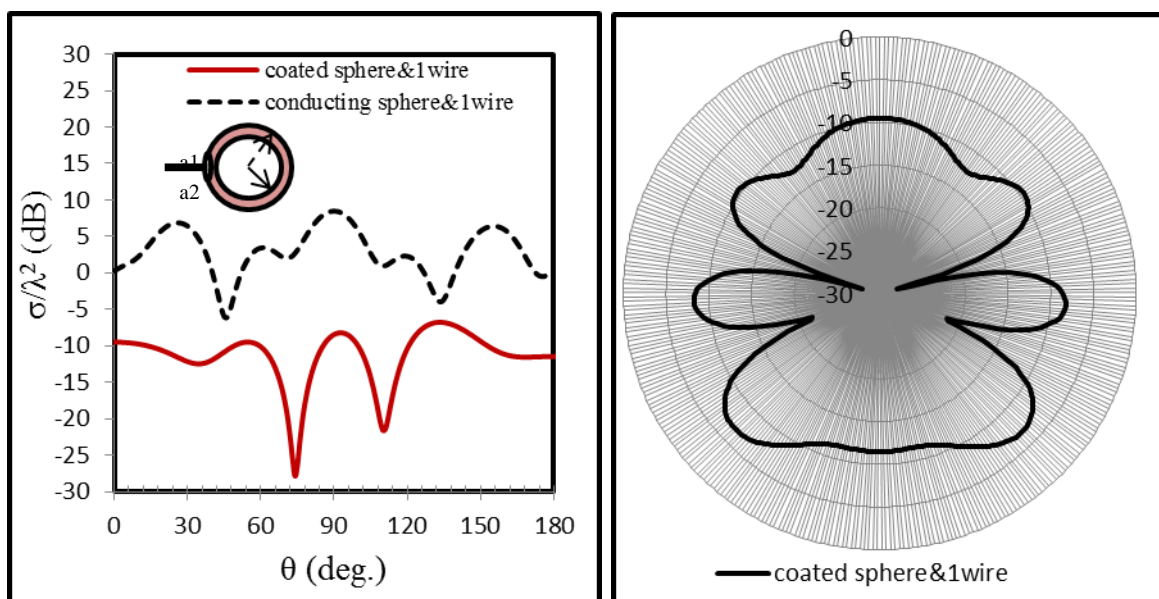


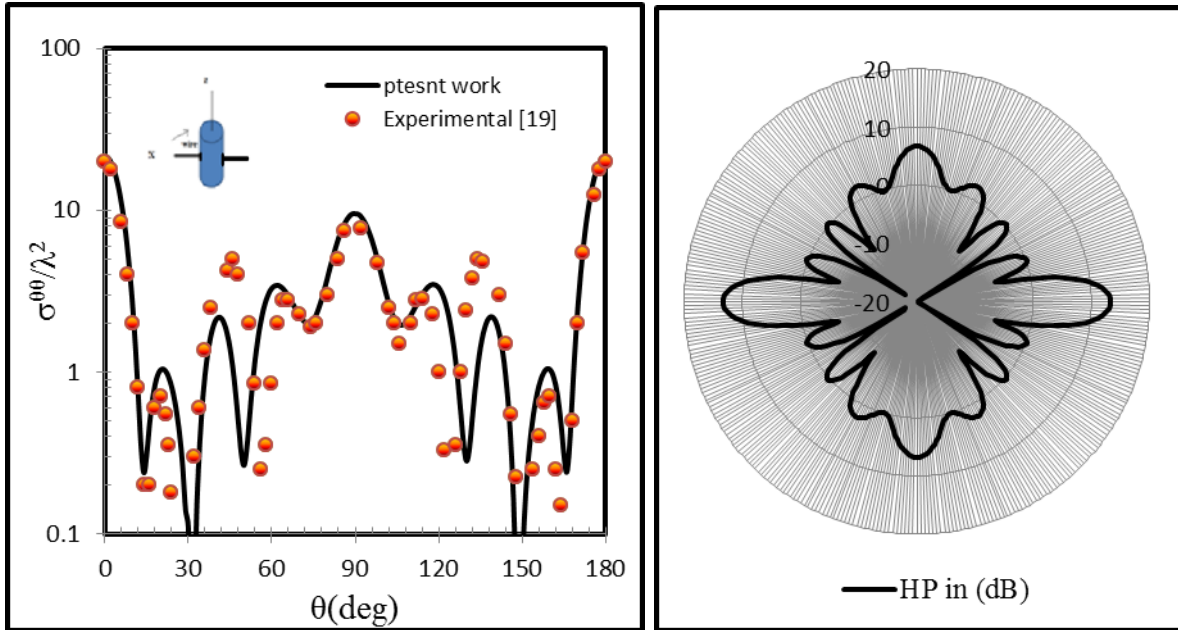
**Fig.(6): (a) Backscattering RCS in HP from conducting sphere ( $a=0.444\lambda$ ) with one attached wire ( $l_w = 0.444\lambda$ ). (b)HP present work with radar graph representation.**



(a)

(b)

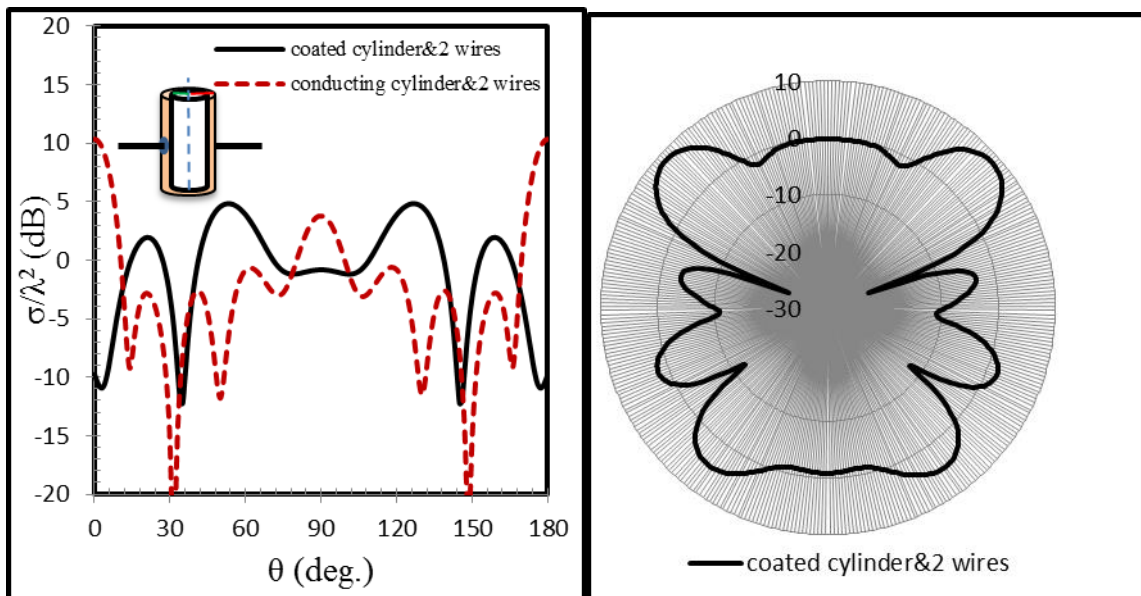
**Fig.(7): (a) Monostatic RCS in HP ( $\phi=0^\circ$ ) for coated sphere with single attached electric wire: comparison with result of conductor case,  $a_1=0.444\lambda$ ,  $a_2=0.361\lambda$ ,  $l_w=0.444\lambda$ ,  $\epsilon_r=4$ . (b) radar graph representation .**



( a )

( b )

**Fig.(8): (a) Monostatic RCS in HP from conducting cylinder ( $a=0.344\lambda$ ,  $l_c = 1.98\lambda$ ) with two attached wire ( $l_{w1} = l_{w2} = 0.880\lambda$ ) (b)HP present work with radar graph representation.**



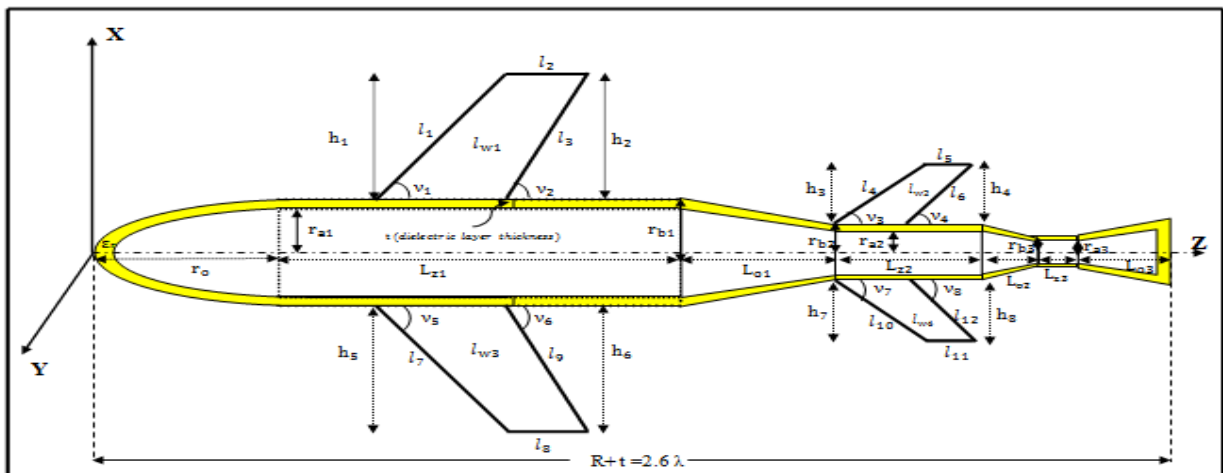
(a)

(b)

**Fig.(9): (a) Monostatic RCS in HP ( $\phi=0^\circ$ ) for coated cylinder with two attached electric wire: comparison with result of conductor case,  $a_1=0.344\lambda$ ,**

$a_2=0.261\lambda$ ,  $l_w=0.880\lambda$ ,  $\epsilon_r=4$ . (b) radar graph representation for coated sphere and two wires.

Third application involves the complex irregular shapes structure with complex geometry as a proposed model of the conducting and coated BOR with attached wires. DCBOR (rocket) with four electric wings is used with same ideal dimensions in CBOR, where the engineering scheme depicted in Figure(10). From this scheme, we find that the rocket body without wings (BOR) consisting of three cylinders are separated from each other by three conical parts, in addition to the spherical front end



of the rocket. All these parts have a total length fixed  $2.6\lambda$ .

**Fig.(10 ):** Geometric scheme to parts of the DCBOR with four conducting wings as proposed model.

For the BOR we have the following structural formula:  $R=2.6\lambda=9.2*a+27.5*L$   
Where,  $a=0.118\lambda$  and the BOR parts have the Measurements insert in table (1).

**Table (1):** Dimensions of BOR parts in term of reference ratio a, and L.

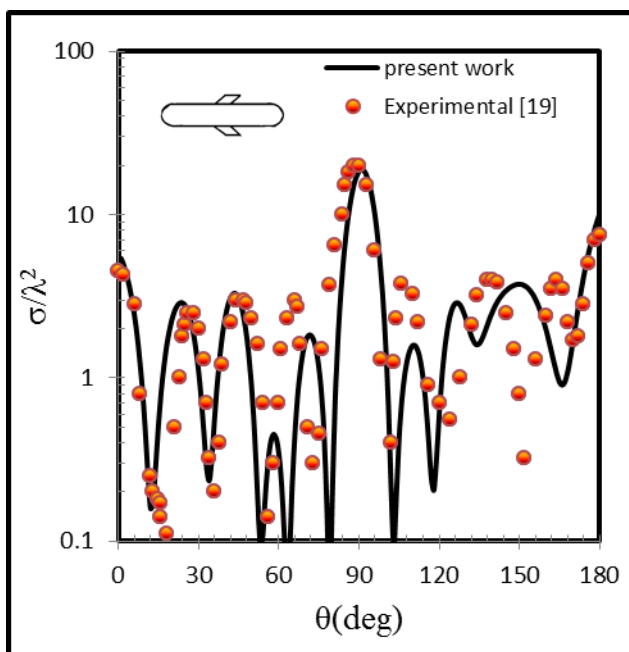
Dimensio ns	$r_o$	$r_{a1}$	$r_{a2}$	$r_{a3}$	$L_{z1}$	$L_{z2}$	$L_{z3}$	$L_{o1}$	$L_{o2}$	$L_{o3}$
value	2.7*	2.7*	1.8*	1.0*	22.4*	4.3*	0.8*	4.1*	0.6*	1.8*
	a	a	a	a	L	L	L	a	a	a

These measurements give a perfect shape for a rocket BOR by choosing the value of **a** and **L** as a reference ratio. As for choosing the ideal measurements of the wings will come as in table (2):

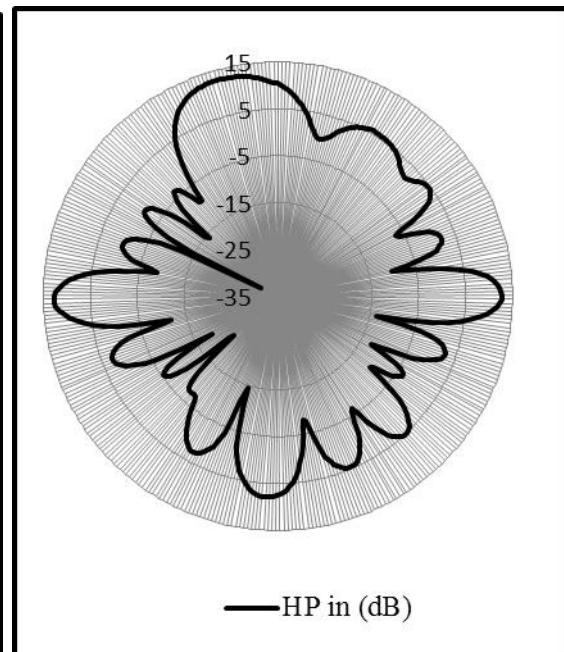
**Table (2): Dimensions of wings in term of large parts of BOR.**

Case	Large wings Dimensions			Small wings Dimensions		
	$l_1=l_7$	$l_2=l_8$	$l_3=l_9$	$l_4=l_{10}$	$l_5=l_{11}$	$l_6=l_{12}$
In term of large radius	$4.*r_o$	$0.78* r_o$	$3.815* r_o$	$1.555* r_o$	$0.35* r_o$	$1.444* r_o$
In term of large cylinder	$1.034*L_z$	$0.2* L_{z1}$	$0.986*L_z$	$0.402*L_{z1}$	$0.0935*L_{z1}$	$0.373*L_z$
In term of large radius and cylinder	$4.* r_o$	$0.2*L_{z1}$	$3.815* r_o$	$1.555* r_o$	$0.0935*L_{z1}$	$1.444* r_o$

the formulations are generalize for the proposed model by comparison with composite body, that was represented by a missile with two identical slant wings. The missile satisfy a good convergence with measurement [19] as shown in figure(11). The RCS for the rocket approximate to this body depicted in Figure (12) and from through it a convergence in HP except some difference which comes from the flat end of the rocket body and the number of wings.



( a )



( b )

**Fig.(11):(a)Monostatic RCS in HP from cylinder with hemisphere endcaps and wire-loop wings ( $ka=2.16$ ,  $L = 2.6\lambda$ ,  $l_{w1}=l_{w2}=0.826\lambda$ ,  $l_2=0.76 l_1$  and  $v_1=45^\circ$  ).**  
**(b)HP present work with radar graph representation.**

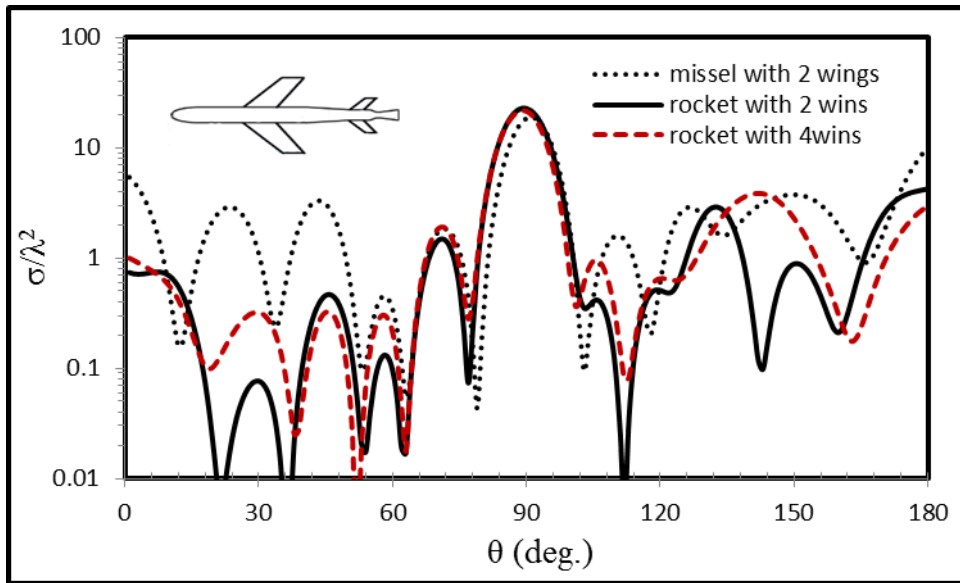


**Fig.(12): Monostatic RCS in HP ( $\phi=0^\circ$ ) of Fig.(10) for the conductor case in comparison with the missile of Fig.(11).**

Third application includes several effects for coated parameters on total RCS, which means loss mechanisms of RAM parameters, and can be incorporated as follows:

1- Figure (13) shows the effect of the dielectric constant, with single layer of constant thickness ( $t=0.083\lambda$ ), on the RCS pattern. It can be shown that the effect of this parameter ( $\epsilon_r$ ) is very clear on RCS pattern when the dielectric constant varied, comparing with that of the conducting rocket case.

2- The thickness of dielectric layer is taken as an effective variable parameters for reducing RCS pattern. Figure(14) illustrates monostatic RCS results as a function of different layer thickness and constant  $\epsilon_r$ . It was shown from this figure that the dielectric layer thickness ( $t$ ) can be verifying to get results for decreasing in most parts and increasing in some parts,  $\theta > 90^\circ$ , of RCS in comparison with conducting case.

3- An application of RAM coated aircraft was used by [20], and later used in partial coated by [21]. For a new application the RAM include electric and magnetic absorbing material. Three values of normalized complex permittivity and permeability values  $\epsilon_r$  and  $\mu_r$  were applied on coated layer of rocket BOR. Each value tested to illustrate the impact on RCS as shown in the Figure(15), in which we find a good check for radar cross section reduction (RCSR).

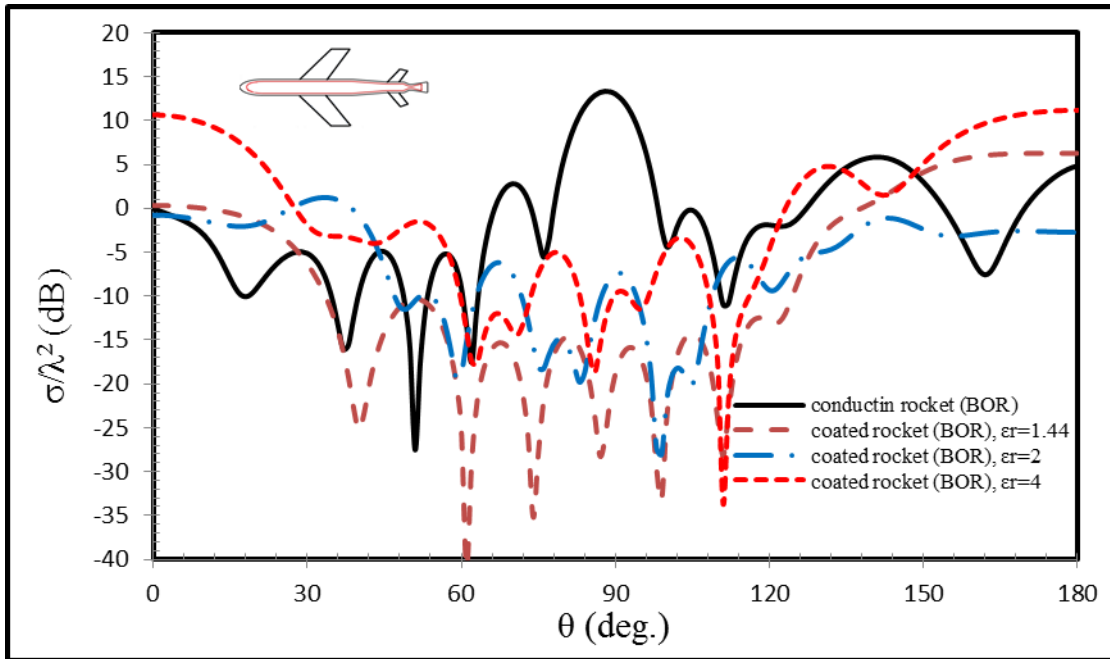


**Fig.(13): Monostatic RCS in HP ( $\phi=0^\circ$ ) of Fig.(10) of dielectric layer thickness,  $t=0.083\lambda$ , as a function of dielectric constant  $\epsilon_r$ , in comparison with the result of conductor case.**

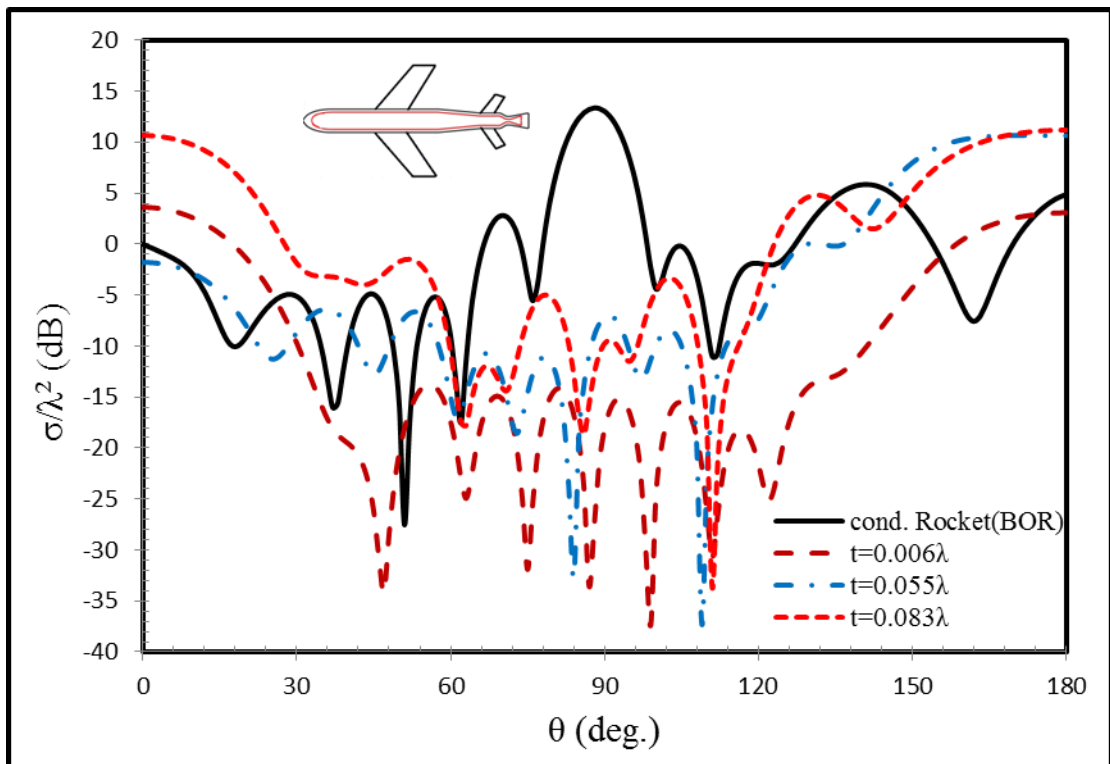


**Fig.(14): Monostatic RCS in HP ( $\phi=0^\circ$ ) of Fig.(10) of dielectric constant  $\epsilon_r=4$ , as a function of layer thickness (t), in comparison with the result of conductor case.**

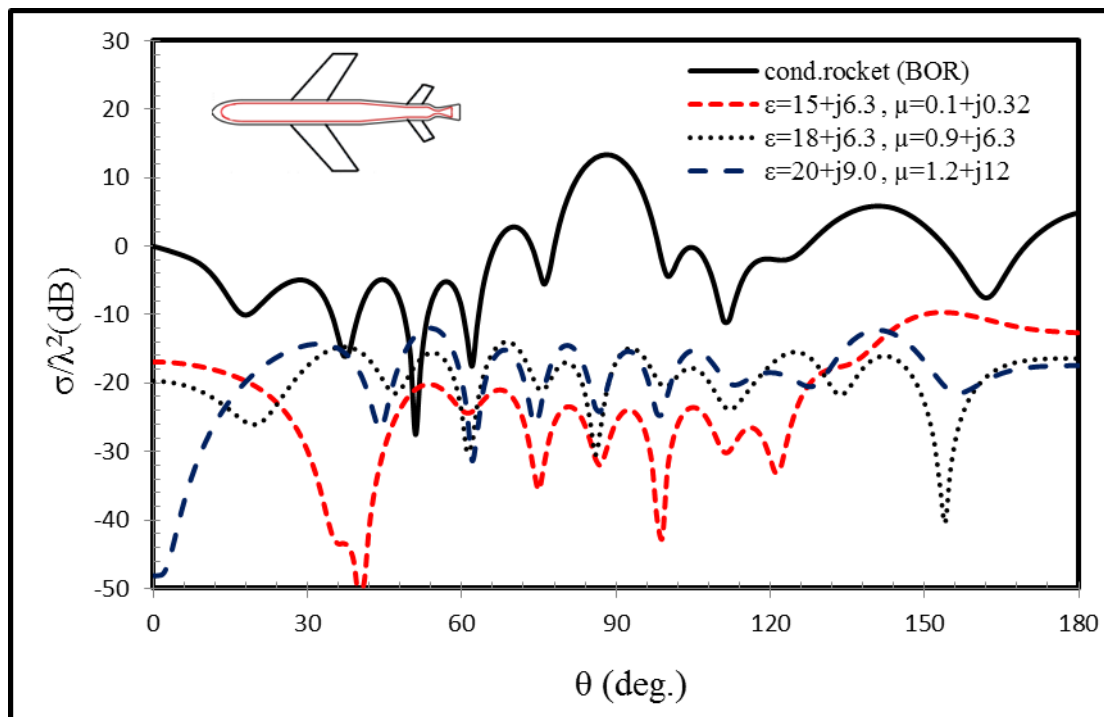


**Fig.(15): Comparison of Monostatic RCS in HP ( $\phi=0^\circ$ ) for geometry in Fig.(10) of dielectric layer thickness,  $t=0.083\lambda$ , as a function of complex lossy dielectric constant in which has electric and magnetic RAM , comparison with the result of conductor case.**

## Conclusions

The analytical treatment of this work enables us to include the effects of the attached wires on the BOR radar cross section, where the addition of attached wires significantly alters the constant CBOR and DCBOR cross-section.

The EM scattering from coated conducting BOR with attached wires was solved using EFIE-PMCHWT formulations generated by surface integral equations. The computational technique of solving the EFIE-PMCHWT by the MoM is shown here to be applicable to scattering problems. They gave excellent results compared with the experimental results available in the case of the conductor body with attached wires.

The formulations are valid for coated conducting BOR. They can

therefore be used to investigate and ensure the solution accuracy of composed body problems, and then the proposed model. The performance of formulations was appeared clearly. In particular, the thickness of the coating layer is an important factor for the attenuation of EM waves, and it showed in the reduce of RCS for different values of thickness. Moreover, Coated with single dielectrically layer in proposed model, DCBOR-wire-junction, is treated efficiently with that formulations, where the reducing in RCS pattern has greatly influenced.

The results indicate that, the using of RAM include complex parameters  $\epsilon$  and  $\mu$ , for electric and magnetic absorbing materials, with single layer of constant thickness ( $t=0.083\lambda$ ), was a good check for RCSR in partial coated in complex and irregular proposed model. Where this method has proven its efficiency in reducing and distortion the RCS pattern.

### References

- [1] Yehuda, L., Amir, B. and Alona, B., "**Analysis of electromagnetic scattering from dielectrically coated conducting cylinders using a multifilament current model**", IEEE Trans. Antennas. Propagat. Vol. 36, No. 11, 1988.
- [2] Kishk, A. A., and Shafai, L., "**Numerical solution of scattering from coated bodies of revolution using different integral equation formulations**", IEE Proc. Vol. 133, Pt. H, No. 3, pp. 227-232, 1986.
- [3] Putnam, J. M., and Medgyesi-Mitschang, L. N., "**Combined field integral equation formulation for inhomogeneous two-and three-dimensional bodies: the junction problem**", IEEE Trans. Antennas Propaga., Vol.39, No. 5, 1991.
- [4] Kishk, A. A., and Gordon, R. K., "**Electromagnetic scattering from conducting bodies of revolution coated with thin magnetic materials**", IEEE Trans. on Magnetics, Vol. 30, No. 5, 1994.
- [5] Yang, H., Xia, Y., Shu, L. and Wu, L., "**Electromagnetic scattering from conducting flat plates coated with thin RAM**", Wuhan University Journal of Natural sciences, Vol. 7, No. 2, pp.185-188, 2002.
- [6] Lei, L., Hu, J., and Hu, H., "**Solving scattering from conducting body coated by thin-layer material by hybrid shell vector element with boundary integral method**", Int. Jour. Antennas Propaga., Research Article, Artical ID 854647, 2012.

- [7] Rao, S. M., Chung, C. C., Cravey, L. R., and Wilkes, D. L., **"Electromagnetic scattering from arbitrary shaped conducting bodies coated with lossy materials of arbitrary thickness"**, IEEE Trans. Antennas Propag., Vol. 39, No. 5, 1991.
- [8] Mautz, J. R., and Harrington, R. F., **"H-field, E-field, and combined field solutions for bodies of revolution"**, Interim Technical Report, RADC-TR-77-109, 1977.
- [9] Harrington, R. F., **"Field Computation by Moment Methods"**, Macmillan, New York, 1968.
- [10] Stutzman, W. L., and Thiele, G. A., **"Antenna theory and design"**, John Wiley & Sons, Inc., New York, 1981.
- [11] Junker, G. P., Kishk, A. A., Glisson, A. W., and Kajfez, D., **"Dielectric disk radiating elements"**, Rome Lab., Technical Report, RL-TR-95-149, University of Mississippi, 1995.
- [12] Huddleston, P. L., Medgyesi-Mitschang, L. N., and Putnam, J. M., **"Combined field integral equation formulation for scattering by dielectrically coated conducting bodies"**, IEEE Trans. Antennas Propag., Vol. AP-34, No. 4, pp. 510-520, 1986.
- [13] Medgyesi-Mitschang, L. N. and Putnam, J. M., **"Electromagnetic scattering from axially inhomogeneous bodies of revolution"**, IEEE Trans. Antennas Propag., vol. AP-32, No.8, 1984.
- [14] Wu, T. K., and Tsai, L. L., **"Scattering from arbitrarily-shaped lossy dielectric bodies of revolution"**, Radio Science, Vol.12, No.5, pp.709-718, 1977
- [15] Shaeffer, J. F. and Medgyesi-Mitschang, L. N., **"Radiation from wire antennas attached to bodies of revolution: the junction problem"**, IEEE Trans. Antennas Propag., Vol. AP-29, No. 3, 1981.
- [16] Cao, X., and Gao, J., **"The singularity problem at the wire/surface junction region for antenna and arrays with bodies of revolution"**, Prog. Electromagn. Research B., Vol.10, 117-130, 2008.
- [17] Newman, E. H., and Pozar, D. M., **"Electromagnetic modeling of composite wire and surface geometries"**, IEEE Trans. Antennas Propag., Vol. AP-26, No.6, 1978.
- [18] Harrington, R. F. and Mautz, J. R., **"Radiation and scattering from bodies of revolution"**, Rep.. AFCRL-69-0305, Syracuse Univ., Syracuse. NY, 1969.
- [19] Shaeffer, J. F., **"EM scattering from bodies of revolution attached wires"**, IEEE Trans. Antennas Propag., Vol. AP-30, No. 3, 1982.

[20] Knott, E .F., Shaeffer, J. F., and Tuley, M.T., "**Radar Cross Section, 2nd Edition**", Sci.Tech Publishing, Inc. 2004.

[21] Mauro, A. A., Rafael, J. P., and Mirabel, C. R., "**Simulations of the radar cross section of stealth aircraft**", SBMO/IEEE MTT-S International Microwave & optoelectronics Conference, pp.409-412, IMOC 2007.